



# Solid Polymer Electrolytes Based on Copolymers of Cyclic Carbonate Acrylate and *n*-Butylacrylate

Fadoi Boujioui, Helen Damerow, Flanco Zhuge, and Jean-François Gohy\*

Solid polymer electrolytes (SPEs) are prepared by mixing poly(2-oxo-1,3-dioxolan-4-yl)methyl acrylate-*random-n*-butylacrylate) [P(cyCA-*r*-*n*BA)] statistical copolymers with bis(trifluoromethane)sulfonimide lithium salt. The P(cyCA-*r*-*n*BA) copolymers are synthesized by reversible addition-fragmentation chain transfer polymerization and different molar masses as well as copolymer composition are targeted in order to study the influence of the molecular parameters on the thermal, mechanical, and electrochemical properties of the SPEs obtained after mixing the copolymers with lithium salts. In the investigated experimental window, it is shown that the thermal and mechanical properties of the SPEs mainly depend on the composition of the copolymer and are poorly influenced by the molar mass. In sharp contrast, the ionic conductivities are more deeply influenced by the molar mass than by the composition of the copolymers. In this respect ionic conductivity values ranging from  $4.2 \times 10^{-6} \text{ S cm}^{-1}$  for the lower molar mass sample to  $8 \times 10^{-8} \text{ S cm}^{-1}$  for the higher molar mass one are measured at room temperature for the investigated SPEs.

and increasing the glass transition temperature ( $T_g$ ) of the polymer.<sup>[6]</sup> As a result, solid-state batteries using PEO-based SPEs should be operated above the melting temperature of PEO, typically around 70 °C.<sup>[7]</sup> Therefore, many studies are being conducted to find alternatives to PEO.<sup>[8]</sup>

The carbonate functional groups are known to present high dipolar moment and dielectric constant enabling them to dissociate many types of salts.<sup>[9]</sup> They are found especially as five-membered cycles in the composition of commercial liquid electrolytes, ethylene, and propylene carbonate being representative examples. Carbonates were thus introduced into polymeric architectures in order to provide polymer electrolytes as demonstrated by the early work of Tarascon and co-workers.<sup>[10]</sup> Contrary to the ethylene oxide (EO) units, the carbonate units show a weak coordination with  $\text{Li}^+$  ions.

## 1. Introduction

Improvement of the ionic conductivity of solid polymer electrolytes (SPEs) is an important requirement for the development of safer, flexible, and performant energy storage devices.<sup>[1]</sup> Since poly(ethylene oxide) (PEO) mixed with lithium salts was reported as a promising solid polymer electrolyte,<sup>[2]</sup> many studies have been realized on the nature and the design of ionically conducting polymers in order to improve the solubility of lithium salts in the polymer matrix and the mobility of lithium ions.<sup>[3]</sup> It is known that ion conduction not only depends on the motions of polymer chains (or polymer chain segments) but also on the interactions between the units of the chains and the dissolved salts.<sup>[4]</sup> In this respect, the segmental motion of PEO chains, which allows the migration of ions, essentially takes place in amorphous regions and is hampered in crystalline domains.<sup>[5]</sup> Moreover, the electron-donor oxygen atoms trap and coordinate  $\text{Li}^+$  cations, inhibiting their displacement

Polymers based on cyclic carbonates were essentially investigated as gel polymer electrolytes (GPEs) (i.e., with the presence of liquid electrolytes), whereas the polymer based on noncyclic carbonates were investigated as SPEs. Chai et al. polymerized vinylene carbonate to obtain a polymer incorporating the cyclic carbonate function in the polymer backbone, reaching an ionic conductivity of  $5 \times 10^{-4} \text{ S cm}^{-1}$  at room temperature, good mechanical properties, and an electrochemical stability window up to 4.8 V versus  $\text{Li}^+/\text{Li}$ .<sup>[11]</sup> Cyclic carbonates were also introduced in polymer architectures as side-chains as reported by Lex-Balducci and co-workers who copolymerized a cyclic carbonate methacrylate with oligo(ethylene glycol) methyl ether methacrylate and further studied gel polymer electrolyte obtained by swelling the accordingly obtained copolymers in a carbonate-based electrolyte.<sup>[12,13]</sup> A noncyclic poly(propylene carbonate) providing an ionic conductivity of  $10^{-4} \text{ S cm}^{-1}$  at ambient temperature was described by Zhang et al.<sup>[14]</sup> Tomi-naga and co-workers synthesized a noncyclic poly(ethylene carbonate) and further developed a hybrid membrane based on porous polyimide matrix, supporting a poly(ethylene carbonate)-based SPE reaching an ionic conductivity of  $10^{-5} \text{ S cm}^{-1}$  at 30 °C.<sup>[15,16]</sup> They also proved that the noncyclic poly(ethylene carbonate) could act as a suitable SPE, exhibiting high lithium transference number and high ionic conductivity that increases with the concentration of salts.

Unfortunately, polycarbonates have higher  $T_g$  than polyethers (such as PEO), generating low segmental motion of the chains, which is unfavorable for a good ionic conduction.

Dr. F. Boujioui, H. Damerow, Dr. F. Zhuge, Prof. J.-F. Gohy  
Institute of Condensed Matter and Nanosciences (IMCN)  
Université catholique de Louvain  
Place L. Pasteur 1, 1348 Louvain-la-Neuve, Belgium  
E-mail: jean-francois.gohy@uclouvain.be

 The ORCID identification number(s) for the author(s) of this article can be found under <https://doi.org/10.1002/macp.201900556>.

DOI: 10.1002/macp.201900556

Tominaga and co-workers developed a copolymer composed of noncyclic carbonate and ether units, which was obtained by polymerization of EO with CO<sub>2</sub>.<sup>[17]</sup> The accordingly obtained copolymer presents a low  $T_g$  of 1 °C, an ionic conductivity of 0.48 mS cm<sup>-1</sup>, and a lithium transference number reaching 0.66 at 60 °C. They also prove that the presence of ethylene carbonate units prevented the complexation of Li<sup>+</sup> ions by EO units. Mecerreyes and co-workers synthesized a series of poly(carbonate-ether) by polycondensation of PEO end-capped diol with dimethyl carbonate and investigated the influence of the different content of EO units as well as the different content of bis(trifluoromethane)sulfonimide lithium salt (LiTFSI) salts.<sup>[18]</sup> They found an optimum SPE exhibiting a high ionic conductivity of  $3.7 \times 10^{-5}$  S cm<sup>-1</sup> with 30 wt% of LiTFSI. Besides the presence of PEO groups, the addition of a low amount of LiTFSI salts (below 40 wt%), decreases the  $T_g$  and breaks PEO crystallinity. More information about solid polymer electrolytes based on polycarbonates can be found in recent reviews.<sup>[19,20]</sup>

We have previously disclosed an SPE based on cyclic carbonate trifluoromethacrylate and vinylidene fluoride units, which exhibits an ionic conductivity of  $2 \times 10^{-4}$  S cm<sup>-1</sup> at room temperature.<sup>[21]</sup> Even if the  $T_g$  of the SPE was observed at 31 °C, the material kept some viscoelasticity, which was demonstrated by oscillatory shear measurements carried out in the linear regime with a strain amplitude  $\gamma$  of 0.03%.

Here, we investigate SPEs based on amorphous poly(2-oxo-1,3-dioxolan-4-yl methyl acrylate-*random-n*-butyl acrylate) P(cyCA-*r-n*BA) statistical copolymers. The polymerization of these copolymers by reversible addition-fragmentation chain transfer (RAFT) is detailed in this paper. The RAFT method has been selected because it allows a controlled radical polymerization of the two comonomers, meaning that copolymer chains with well-defined compositions, molar masses, and low dispersity indices can be obtained through this method. The cyCA comonomer has been selected to afford ionic conductivity after salt loading while the *n*BA comonomer is known to lead to low  $T_g$  amorphous polymers and should therefore allow the formation of soft SPEs with increased ionic mobility. Moreover, thermal, mechanical, and ionic conductivity analyses are carried out in order to understand the effect of the polymer structure on the properties of the accordingly obtained SPEs.

## 2. Experimental Section

### 2.1. Materials

All reagents were used as received. Glycerol 1,2-carbonate (>90%) was bought from Tokyo Kasei Inc. Triethylamine (TEA, ≥99%) and  $\alpha,\alpha'$ -azoisobutyronitrile (AIBN, ≥98%) were purchased from Acros Organics. Acryloyl chloride (≥97%), *n*-butyl acrylate (*n*BA, ≥99%), dimethyl sulfoxide (DMSO, ≥99%), sodium bicarbonate (NaHCO<sub>3</sub>, ≥99.7%), sodium sulfate (Na<sub>2</sub>SO<sub>4</sub>, ≥99.5%), lithium perchlorate (LiClO<sub>4</sub>, battery grade, ≥99.99%), LiTFSI (≥99.95%), and 2-dodecylthiocarbonothioylthio-2-methylpropionic acid (DDMAT, ≥98%) were purchased from Sigma-Aldrich. Dimethyl sulfoxide (DMSO-d<sub>6</sub>, > 99.8%), used for NMR spectroscopy, was purchased from Euriso-top.

### 2.2. Methods

#### 2.2.1. NMR

<sup>1</sup>H and <sup>13</sup>C NMR spectra were acquired on a Bruker Avance II spectrometer (300 or 500 MHz) using DMSO-d<sub>6</sub> as solvent.

#### 2.2.2. Size Exclusion Chromatography (SEC)

Average molar masses ( $M_n$  and  $M_w$ ) and dispersities ( $\bar{D}$ ) were measured on an Agilent SEC system equipped with an Agilent 1200 pump; an Agilent differential refractometer and two Polymer Standards Service Gram columns (1000 and 100 Å). *N,N*-dimethylformamide containing  $2.5 \times 10^{-3}$  M of NH<sub>4</sub>PF<sub>6</sub> was used as eluent thermostated at 35 °C with a flow rate of 1 mL min<sup>-1</sup>. The calibration was performed using polystyrene standards.

#### 2.2.3. Differential Scanning Calorimetry (DSC)

DSC measurements were carried out using a Mettler Toledo 822e calorimeter. The samples were analyzed under nitrogen atmosphere in a 40  $\mu$ L Al pan with an empty Al pan as reference cell. The samples were first heated from 25 to 200 °C and cooled down from 200 to -120 °C at a heating rate of 10 °C min<sup>-1</sup>. The temperature was maintained for 2 min before changing cycle. The samples were then heated from -120 to 200 °C at the same heating rate to determine the glass transition temperature ( $T_g$ ) using the Stare software.

#### 2.2.4. Electrochemical Measurements

Thick electrolyte films were prepared as follows. The P(cyCA-*r-n*BA) and LiTFSI salt were dissolved in acetonitrile. This latter was removed under reduced pressure following by the vacuum at 70 °C overnight. The viscous samples were casted on stainless steel electrodes. The thickness was kept constant with a 270  $\mu$ m thick polytetrafluoroethylene spacer placed between two stainless steel electrodes into the Swagelok cell. Electrochemical impedance spectroscopy (EIS) measurements were performed using a Parstat 4000 apparatus over a frequency range of 1 MHz to 10 mHz and with an amplitude a.c. excitation voltage of 5 mV. The temperature dependence measurements were carried out from 22 to 80 °C by gradually increasing the temperature by steps of 10 °C with an equilibration time of  $\approx$ 1 h between each step.

#### 2.2.5. Rheology

Rheological experiments were performed on an Ares (TA Instruments) rheometer equipped with an air/nitrogen convection oven that ensures an accurate temperature control ( $\pm$ 0.1 °C). Dynamic mechanical measurements were carried out at given temperatures, using stainless steel 8 mm cone-plate geometries. The cone geometry has an angle of 0.1 rad and a truncation of 31  $\mu$ m. The sample was equilibrated in the rheometer at

80 °C for 30 min. Dynamic frequency sweeps were performed at a deformation amplitude of 3% at 30 °C under nitrogen atmosphere and a frequency range of 100–0.01 rad s<sup>-1</sup>. All dynamic measurements were performed within the linear viscoelastic region, which was determined from dynamic strain sweep experiments. The equilibration was checked with dynamic time sweep measurements up to 30 min. Normal forces were checked to be relaxed prior any measurement.

### 2.3. Synthetic Procedures

#### 2.3.1. Synthesis of 2-Oxo-1,3-dioxolan-4-yl Methyl Acrylate (cyCA)

Into a 250 mL round-bottom flask, glycerol 1,2-carbonate (10.0 g, 84.68 mmol) and triethylamine (8.74 g, 86.33 mmol) were dissolved in anhydrous dichloromethane (60 mL) and cooled at 0 °C under argon atmosphere. A solution of acryloyl chloride (5.11 g, 56.45 mmol) in dichloromethane (12.0 mL) was added dropwise into the flask and the mixture was left at 0 °C during 1 h before reaching the ambient temperature. After 24 h, the mixture was filtered and then washed with 5% aqueous NaHCO<sub>3</sub> followed by distilled water. The organic phase was dried over Na<sub>2</sub>SO<sub>4</sub> and dichloromethane was removed under reduced pressure. After purification by silica gel column chromatography (hexane: ethyl acetate, 3:2) the product was isolated as a colorless liquid (8.43 g, 53%).

<sup>1</sup>H-NMR (300 MHz, CDCl<sub>3</sub>) δ (ppm): 6.35 (dd, 1H, –HC=CHH, *J* = 16.8, 2.1 Hz), 6.05 (dd, 1H, –HC=CH<sub>2</sub>, *J* = 16.8, 10 Hz), 5.84 (dd, 1H, –HC=CHH, *J* = 10, 2.1 Hz), 4.90 (m, 1H, –O–(CH<sub>2</sub>)CH–CH<sub>2</sub>–, *J* = 7 Hz), 4.52 (t, 1H, –O–CHH–CH–, *J* = 7 Hz), 4.30 (m, 3H, –O–CHH–CH–, and –CH–CH<sub>2</sub>–O–, *J* = 7 Hz).

<sup>13</sup>C-NMR (300 MHz, CDCl<sub>3</sub>) δ (ppm): 165.3 (1C, –HC–CO–O–), 154.5 (1C, –O–CO–O–), 132.3 (1C, CH<sub>2</sub>=CH–), 127.1 (1C, CH<sub>2</sub>=CH–CO–), 73.9 (1C, –O–(CH<sub>2</sub>)CH–CH<sub>2</sub>–), 66.0 (1C, O–CH<sub>2</sub>–CH–), 63.1 (1C, –CH–CH<sub>2</sub>–O).

#### 2.3.2. Synthesis of Poly(2-oxo-1,3-dioxolan-4-yl methyl acrylate) [P(cyCA)]

In a 25 mL flask cyCA (2000 mg, 11.62 mmol, 50 eq.), AIBN (8 mg, 0.05 mmol, 0.2 eq.), and DDMAT (85 mg, 0.23 mmol, 1 eq.) were dissolved in DMSO (11.6 mL). The mixture was purged with argon for 30 min and immersed in a preheated oil bath at 70 °C. After 125 min, the reaction was stopped by cooling in liquid nitrogen and by exposing to air. The polymer was precipitated in ethanol, filtered, and washed with ethanol to obtain P(cyCA)<sub>41</sub>. To determine the final conversion and the dispersity, the analysis was performed by SEC and <sup>1</sup>H-NMR (in DMSO-d<sub>6</sub>).

#### 2.3.3. Typical Procedure for the Synthesis of Poly(2-oxo-1,3-dioxolan-4-yl methyl acrylate-random-*n*-butylacrylate) [P(cyCA-*r*-*n*BA)]

In a 50 mL flask (2-oxo-1,3-dioxolan-4-yl)methyl acrylate (2000 mg, 11.62 mmol, 50 eq.), *n*-butyl acrylate (2000 mg,

4.64 mmol, 20 eq.), AIBN (8 mg, 0.05 mmol, 0.2 eq.), and DDMAT (85 mg, 0.23 mmol, 1 eq.) were dissolved in DMSO (16.2 mL). The mixture was purged with argon for 30 min and immersed in a preheated oil bath at 70 °C. After 90 min, the reaction was stopped by cooling with liquid nitrogen following by exposure to air. The polymer was precipitated in water, filtered, and washed with water and methanol. To determine the final conversion and the dispersity, the analysis was performed by GPC and <sup>1</sup>H-NMR (in DMSO-d<sub>6</sub>). P(cyCA<sub>19</sub>-*r*-*n*BA<sub>35</sub>), P(cyCA<sub>37</sub>-*r*-*n*BA<sub>20</sub>), and P(cyCA<sub>44</sub>-*r*-*n*BA<sub>71</sub>) were obtained by using [cyCA]/[*n*BA]/[DDMAT] molar ratios equal to 30:40:1, 50:20:1, and 60:80:1, respectively.

## 3. Results and Discussion

### 3.1. Synthesis of P(cyCA-*r*-*n*BA) Copolymers via RAFT Polymerization

The cyCA monomer was synthesized in one step, according to the protocol of Yoshikawa et al.<sup>[22]</sup> The synthesis was achieved by esterification of glycerol 1,2-carbonate with acryloyl chloride, which was base-catalyzed with triethylamine in dichloromethane. The cyCA monomer was yielded at 53%.

The cyCA was RAFT homopolymerized in order to be used as reference afterward. The polymerization was performed at 70 °C in DMSO at 1 mol L<sup>-1</sup> with DDMAT as RAFT chain transfer agent (CTA) and AIBN as initiator (**Figure 1**).

The CTA/initiator ratio was kept at 5. In order to study the kinetics of the polymerization, samples of the reaction medium were withdrawn and subjected to <sup>1</sup>H-NMR and SEC analyses. The initiation of the polymerization is slow and only 23% of conversion are reached after 45 min (**Figure 2a**). However, after 125 min of polymerization, the conversion reaches 82%, meaning a relatively fast propagation. Between 45 and 125 min of polymerization, the evolution of Ln[M]<sub>0</sub>/[M]<sub>t</sub> is linear with time, which demonstrates that the concentration of the active propagating species remains constant (**Figure 2a**). Therefore, this indicates that the termination reactions are very low or inexistent. Moreover, the evolution of the molar mass as a function of the conversion is linear, confirming the absence of transfer reactions (**Figure 2b**). Finally, the dispersity keeps narrow values between 1.10 and 1.13 during the polymerization (**Figure 2b**). These results are consistent with SEC curves observed as narrow mono-modal peaks (**Figure 2c**). The RAFT polymerization of cyCA is thus considered as a controlled radical polymerization. In this study, the polymerization was stopped at 82% of conversion, yielding to the desired P(cyCA)<sub>41</sub> homopolymer (**Figure S1**, Supporting Information).

Finally, cyCA was randomly copolymerized with *n*-butyl acrylate (*n*BA) (**Figure 3**). The RAFT copolymerization was

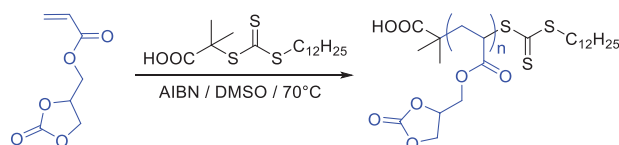


**Figure 1.** RAFT homopolymerization of cyCA.

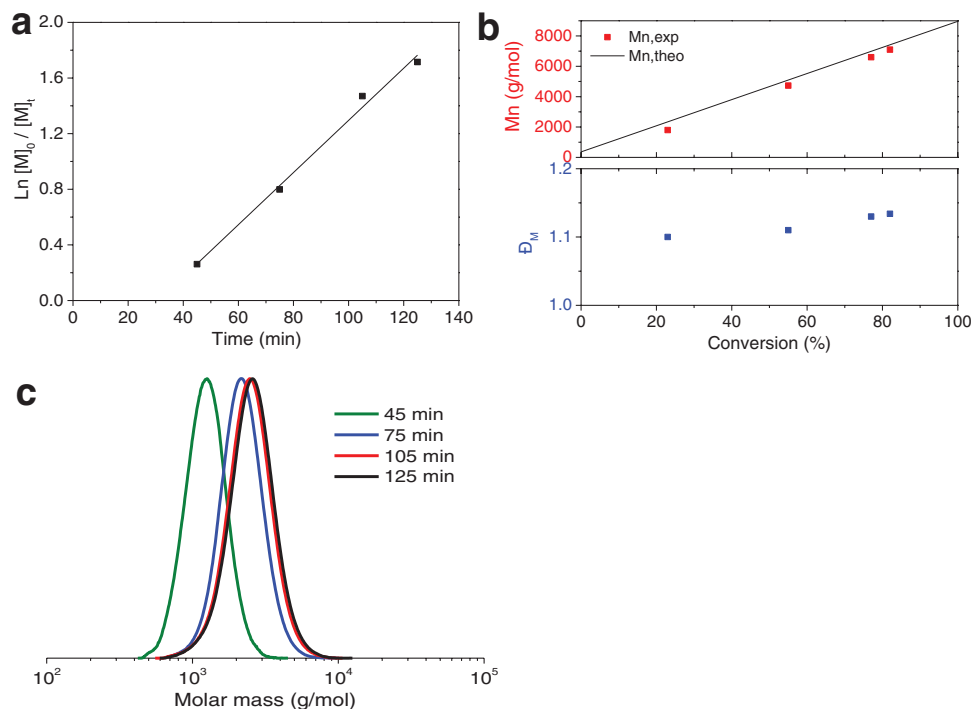


**Figure 2.** a) Dependence of  $\text{Ln}[M]_0/[M]_t$  versus time, b) dependence of  $M_n$  and of dispersity ( $\bar{D}_M$ ) versus conversion, and c) evolution of the molar mass with polymerization time for the homopolymerization of cyCA.

conducted under the same conditions and with the same reagents that for the  $\text{P}(\text{cyCA})_{41}$  homopolymer. Three different copolymers with various monomer compositions and various chain lengths were synthesized:  $\text{P}(\text{cyCA}_{19}\text{-}r\text{-}n\text{BA}_{35})$ ,  $\text{P}(\text{cyCA}_{37}\text{-}r\text{-}n\text{BA}_{20})$ , and  $\text{P}(\text{cyCA}_{44}\text{-}r\text{-}n\text{BA}_{71})$ , the numbers in subscripts representing the average degree of polymerization of the corresponding blocks as determined by  $^1\text{H-NMR}$ .

The SEC analyses (**Figure 4**) show shifting of narrow monomodal peaks toward higher molar mass, proving that copolymerization is taking place. The evolution of molar mass obtained by SEC is in correlation with the trends obtained by NMR. Moreover, the  $\text{P}(\text{cyCA}_{19}\text{-}r\text{-}n\text{BA}_{35})$ ,  $\text{P}(\text{cyCA}_{37}\text{-}r\text{-}n\text{BA}_{20})$ , and  $\text{P}(\text{cyCA}_{44}\text{-}r\text{-}n\text{BA}_{71})$  random copolymers display a dispersity ( $\bar{D}$ ) of 1.15, 1.18, and 1.23, respectively. Thus, the dispersity increases when high molar masses are targeted is in line with a possible loss of control for the RAFT copolymerization.

To summarize, four polymers based on cyCA units were synthesized by RAFT and are reported in **Table 1**. The  $\text{P}(\text{cyCA})_{41}$  homopolymer is used as reference with a cyCA content of 100 wt%. The three others are based on a mix of cyCA and *n*BA monomers. In order to study the influence of the composition

in cyCA and *n*BA on ionic conductivity measurements, two copolymers were synthesized with a similar chain length but a different cyCA content. These are the  $\text{P}(\text{cyCA}_{19}\text{-}r\text{-}n\text{BA}_{35})$  and  $\text{P}(\text{cyCA}_{37}\text{-}r\text{-}n\text{BA}_{20})$  copolymers which present approximately the same molar mass, 8200 and 8700  $\text{g mol}^{-1}$ , respectively. However, the  $\text{P}(\text{cyCA}_{19}\text{-}r\text{-}n\text{BA}_{35})$  contains 42 wt% of cyCA, whereas the  $\text{P}(\text{cyCA}_{37}\text{-}r\text{-}n\text{BA}_{20})$  has 71 wt%. On the other hand, to observe the influence of the chain length, two other copolymers display similar cyCA content but different molar masses. In this respect, the  $\text{P}(\text{cyCA}_{44}\text{-}r\text{-}n\text{BA}_{71})$  copolymer is comprising 45 wt% of cyCA like the  $\text{P}(\text{cyCA}_{19}\text{-}r\text{-}n\text{BA}_{35})$ , but it is ca. two times longer than the latter.

### 3.2. Thermal Properties

The glass transition temperatures were measured using DSC. The  $T_g$  of the  $\text{P}(\text{cyCA})$  is measured at 68 °C (**Figure 5**). In order to prepare SPEs, cyCA-containing polymers are mixed with lithium salts. Therefore, we have investigated the effect of the nature of the salt on the thermal properties of the investigated

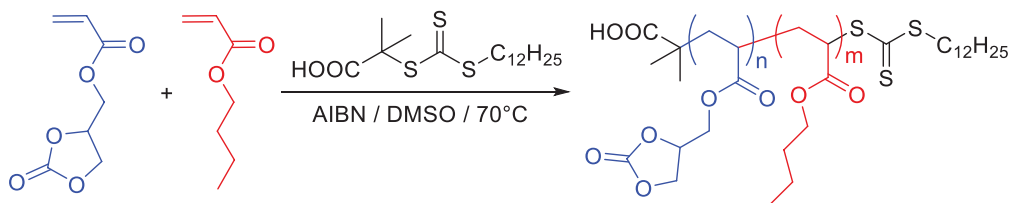


**Figure 3.** Synthesis of poly(2-oxo-1,3-dioxolan-4-yl methyl acrylate-*r*-*n*butyl acrylate) via RAFT [ $\text{P}(\text{cyCA}\text{-}r\text{-}n\text{BA})$ ].

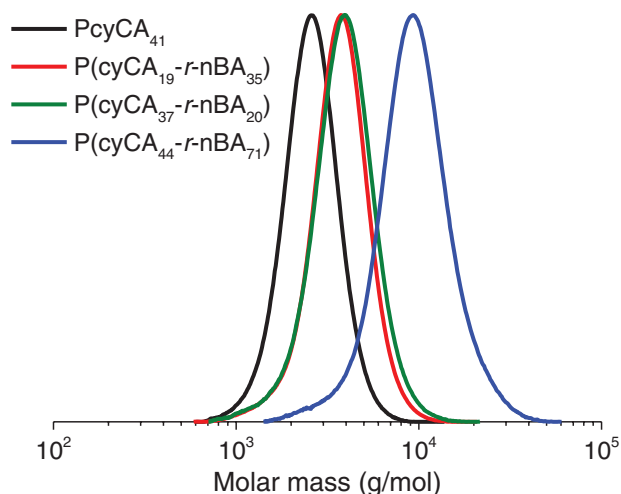


**Figure 4.** SEC curves superposition of homopolymer and copolymers based on cyCA.

(co)polymers. In this respect, DSC measurements were first performed on  $P(\text{cyCA})_{41}$  with two different added salts, namely  $\text{LiClO}_4$  and  $\text{LiTFSI}$  (Figure 5). These salts are often used in order to prepare SPEs.<sup>[1–7]</sup> The  $\text{cyCA}/\text{Li}^+$  ratio was kept at 5 for both the used salts, a ratio commonly used in SPEs.<sup>[1–7]</sup>

We observe that the  $T_g$  varies with the addition of salt and that the nature of the anion plays an important role. More precisely, the use of  $\text{LiTFSI}$  leads to a decrease in the  $T_g$  from 68 to 63 °C, while  $\text{LiClO}_4$  increases it to 81 °C. This can be explained by the fact that the volume of the  $\text{TFSI}^-$  anion is higher than the volume of the  $\text{ClO}_4^-$  anion, leading to the formation of free volume between the chains and hence decreasing the value of the  $T_g$ .<sup>[23]</sup> As a result, the polymer chains are expected to be more mobile in the presence of  $\text{LiTFSI}$  than  $\text{LiClO}_4$  and this should have a positive impact on the ionic mobility of lithium ions. This effect has been already observed for PEO-based SPEs.<sup>[23]</sup> Moreover, the larger size of  $\text{TFSI}^-$  anions compared to  $\text{ClO}_4^-$  ones is leading to a better separation with  $\text{Li}^+$  cations and an increased ionic conductivity for the system since  $\text{Li}^+$  cations can move more freely. Thus, only  $\text{LiTFSI}$  was considered thereafter.

The poly(*n*BA) homopolymer is characterized by a  $T_g$  of –54 °C. Thus, the addition of *n*BA monomer solely decreases the  $T_g$  of the  $P(\text{cyCA}-r\text{-}n\text{BA})$  copolymers (Figure 6).

The  $P(\text{cyCA}_{19}\text{-}r\text{-}n\text{BA}_{35})$ , which has the same chain length than  $P(\text{cyCA}_{37}\text{-}r\text{-}n\text{BA}_{20})$ , displays the lowest  $T_g$  (Figure 6a). Therefore, the  $T_g$  of copolymers decreases from of 26 to 1 °C when the *n*BA content increases from 29 to 58 wt%. These

**Table 1.** Summary of (co)polymers characteristic features.

Sample	vcyCA content (wt%)	$M_n^a$ [g mol <sup>-1</sup> ]	$\mathcal{D}^b$
$P(\text{cyCA})_{41}$	100	7400	1.13
$P(\text{cyCA}_{19}\text{-}r\text{-}n\text{BA}_{35})$	42	8200	1.15
$P(\text{cyCA}_{37}\text{-}r\text{-}n\text{BA}_{20})$	71	8700	1.18
$P(\text{cyCA}_{44}\text{-}r\text{-}n\text{BA}_{71})$	45	16 900	1.24

<sup>a</sup>Determined by <sup>1</sup>H NMR; <sup>b</sup>Determined by SEC.

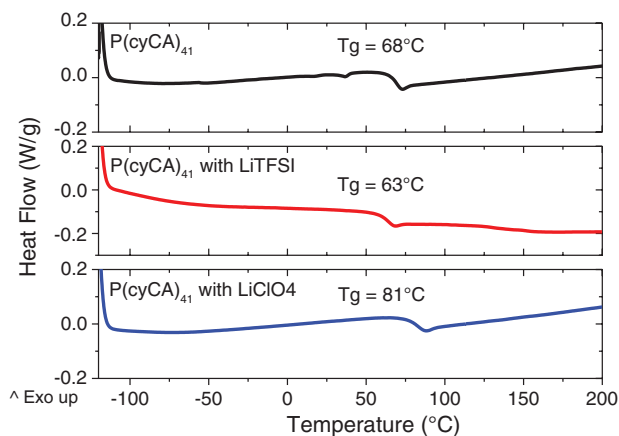


**Figure 5.** DSC thermograms of  $P(\text{cyCA})_{41}$  without salt, with  $\text{LiTFSI}$ , and with  $\text{LiClO}_4$  (at  $\text{cyCA}/\text{Li}^+$  ratio of 5).

observations are in line with the fact that the chemical nature of the monomers as well as the composition of the copolymers influences the thermal properties of the materials. Although

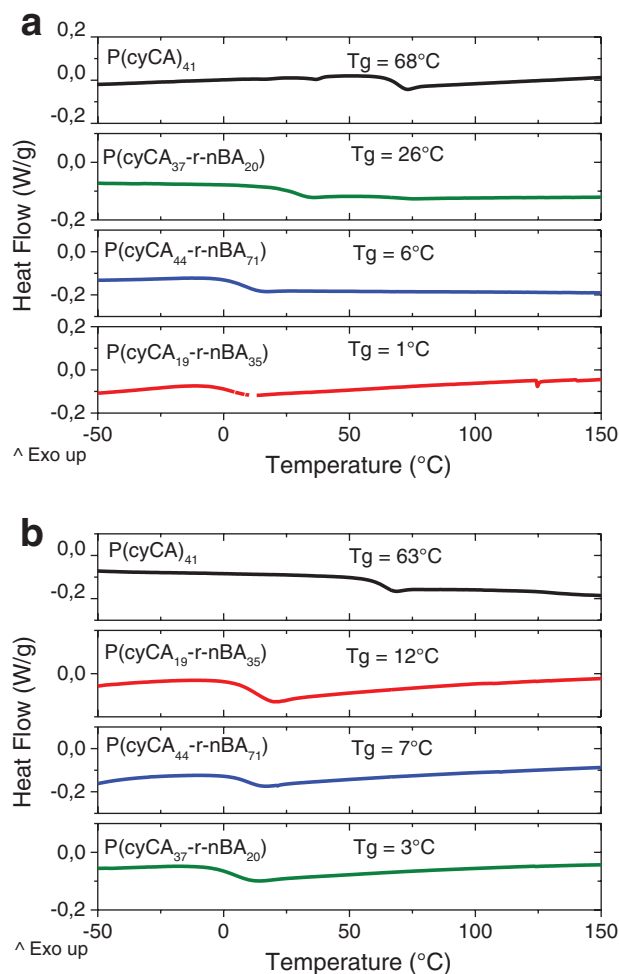


**Figure 6.** DSC thermograms of homopolymer and copolymers based on cyCA: a) without  $\text{LiTFSI}$  salt and b) with  $\text{LiTFSI}$  salt (at  $\text{cyCA}/\text{Li}^+$  molar ratio = 5).

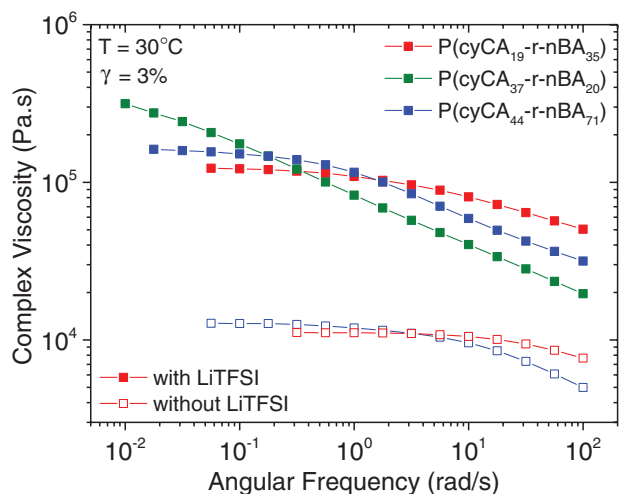


**Figure 7.** Complex viscosity  $\eta^*$  (Pa s) versus angular frequency ( $\text{rad s}^{-1}$ ) for the copolymers with and without LiTFSI (cyCA/Li<sup>+</sup> molar ratio = 5) at 30 °C.

Fox's law is not strictly respected, the fact that one single  $T_g$  has been observed for all the synthesized copolymers and that its value decreases when the content of the low  $T_g$  component  $n$ BA increases points toward a statistical distribution of cyCA and  $n$ BA in the P(cyCA- $r$ - $n$ BA) copolymers. The chain length has only a slight impact on the  $T_g$ . Indeed, for the copolymers composed of  $\approx 43$  wt% of cyCA, such as P(cyCA<sub>19</sub>- $r$ - $n$ BA<sub>35</sub>) and P(cyCA<sub>44</sub>- $r$ - $n$ BA<sub>71</sub>), the  $T_g$  increases only of 5 °C despite the chains are ca. two times longer for the latter sample. The addition of LiTFSI (at cyCA/Li<sup>+</sup> molar ratio = 5) lowers the  $T_g$  of P(cyCA<sub>37</sub>- $r$ - $n$ BA<sub>20</sub>) from 26 to 3 °C, while the  $T_g$  of P(cyCA<sub>19</sub>- $r$ - $n$ BA<sub>35</sub>) increases from 1 to 12 °C (Figure 6b). Thus, the presence of a larger cyCA content increases free volume, allowing the polymer chain segments to move easily. In the presence of LiTFSI, the chain length has again almost no impact on the  $T_g$  (Figure 6b).

### 3.3. Rheological Properties

To investigate the linear viscoelastic properties of copolymers containing LiTFSI, shear rheological experiments were performed. Figure 7 shows the complex viscosity  $\eta^*$  (Pa s) versus angular frequency ( $\text{rad s}^{-1}$ ) for the copolymers without and with LiTFSI (cyCA/Li<sup>+</sup> ratio = 5) at 30 °C (i.e., above their  $T_g$ ).

The  $\eta^*$  of copolymer increases of one decade when the LiTFSI salt is added. Moreover, the flow of the materials is more pronounced with the presence of salts, when the angular frequency increases. In presence of LiTFSI, at low shear frequency (i.e., below  $\approx 10^0 \text{ rad s}^{-1}$ ), the  $\eta^*$  of P(cyCA<sub>19</sub>- $r$ - $n$ BA<sub>35</sub>) and P(cyCA<sub>44</sub>- $r$ - $n$ BA<sub>71</sub>) reaches constant values of  $1.2 \times 10^5$  and  $1.6 \times 10^5$  Pa s, respectively, corresponding to the maximal resistance that the copolymers exhibit under low deformation. The zero-shear viscosity of P(cyCA<sub>44</sub>- $r$ - $n$ BA<sub>71</sub>) is higher than this of P(cyCA<sub>19</sub>- $r$ - $n$ BA<sub>35</sub>). This result is in correlation with the fact that the molar mass is a structural parameter influencing the flow behavior of the copolymer. The zero-shear viscosity of P(cyCA<sub>37</sub>- $r$ - $n$ BA<sub>20</sub>) is

still not observable in the measured angular frequency range. On the contrary, the  $\eta^*$  increases toward infinity. Moreover, at a shear frequency of  $10^{-2} \text{ rad s}^{-1}$ , its  $\eta^*$  is of  $3.2 \times 10^5 \text{ Pa s}$ , which is higher than those of P(cyCA<sub>19</sub>- $r$ - $n$ BA<sub>35</sub>) and P(cyCA<sub>44</sub>- $r$ - $n$ BA<sub>71</sub>). This can indicate that P(cyCA<sub>37</sub>- $r$ - $n$ BA<sub>20</sub>) has a firm texture compared to the other copolymers, which could be due to a high amount of Li<sup>+</sup>-carbonate interactions. At high shear frequency, the three copolymers exhibit shear-thinning flow behavior. The flow of the P(cyCA<sub>37</sub>- $r$ - $n$ BA<sub>20</sub>) is more important than the P(cyCA<sub>44</sub>- $r$ - $n$ BA<sub>71</sub>), which is more important than the P(cyCA<sub>19</sub>- $r$ - $n$ BA<sub>35</sub>). Therefore, the cyCA/Li<sup>+</sup> content has an influence on the mechanical behavior of the copolymer, which is more important than its molar mass.

### 3.4. Ionic Conductivity Measurements

All the copolymers mixed with salts at cyCA/Li<sup>+</sup> molar ratio of 5 were subjected to EIS in order to measure their ionic conductivity. To this aim, the samples were placed between two stainless steel electrodes and the ionic conductivity of samples was measured at various temperatures.

Figure 8 shows the ionic conductivity versus temperature for three copolymers containing LiTFSI. The ionic conductivity of each copolymers decreases linearly with the inverse of temperature. Over the entire measuring temperature range (i.e., from 22 to 80 °C), the P(cyCA<sub>19</sub>- $r$ - $n$ BA<sub>35</sub>) exhibits conductivity values higher than the P(cyCA<sub>44</sub>- $r$ - $n$ BA<sub>71</sub>). At ambient temperature, they display respectively  $4.2 \times 10^{-6}$  and  $8 \times 10^{-8} \text{ S cm}^{-1}$ . Thus, when the molar mass increases, the ionic conductivity decreases. This observation is perfectly in line with previous investigations conducted on copolymer interpenetrating networks containing EO and ethylene carbonate units.<sup>[24]</sup> In this previous report, it was shown that increasing the molar mass of the copolymer resulted in decreased ionic conductivities.<sup>[24]</sup> Concerning the influence of the different amounts of cyCA and  $n$ BA units on the ionic conductivity, we hypothesize that the

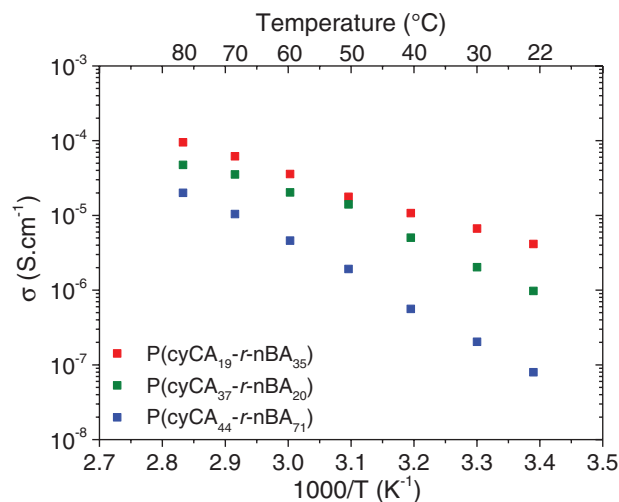


**Figure 8.** Ionic conductivity versus temperature for copolymers based on cyCA and  $n$ BA containing LiTFSI (cyCA/Li<sup>+</sup> molar ratio = 5).

addition of a certain amount of *n*BA units does slightly increase the conductivity by lowering the  $T_g$  of the copolymer. In fact, *n*BA does not contribute directly to the conductivity because it constitutes as “dead” material due to its low polarity. In this respect, we were not able to measure reliable ionic conductivity values for a P*n*BA homopolymer loaded with LiTFSI. Although the P(cyCA<sub>37</sub>-*r*-*n*BA<sub>20</sub>) and the P(cyCA<sub>19</sub>-*r*-*n*BA<sub>35</sub>) contain respectively 71 and 42 wt% of cyCA, their conductivities tend to a constant and seem not to be dependent on the copolymer composition.

#### 4. Conclusions

In this paper, we have prepared SPEs based on amorphous random copolymers, which contain cyclic ethylene carbonate (cyCA) and *n*-butyl acrylate (*n*BA) comonomers. They were easily obtained by RAFT polymerization. Moreover, we demonstrated that the difference in molar mass (i.e.,  $M_n$  of 8200 and 16900 g mol<sup>-1</sup>) of copolymers having the same cyCA and *n*BA content, does not have a big influence on the flow behavior and the glass transition temperature of the SPEs, maybe because of the small gap between their  $M_n$ . However, this small gap is sufficient to influence the ionic conductivity measurements. Finally, the ionic conductivity values remain approximately the same whatever the amount of cyCA in the copolymer. However, investigation of a higher number of copolymers with different compositions would be required to draw a more definitive conclusion.

#### Supporting Information

Supporting Information is available from the Wiley Online Library or from the author.

#### Acknowledgements

The authors are grateful to the Action de Recherche Concertée BATTAB 14/19-057 for financial support. The authors also thank Marie Curie Actions for the Ph.D. thesis funding from the People Program of the European Commission's Seventh Framework Programme (FP7/2007-2013) under Supolen Grant Agreement No. 607937.

#### Conflict of Interest

The authors declare no conflict of interest.

#### Keywords

copolymers, ethylene carbonate, ionic conductivity, *n*-butylacrylate, solid polymer electrolytes

Received: December 14, 2019

Revised: January 22, 2020

Published online:

- [1] M. Armand, J. M. Tarascon, *Nature* **2008**, *451*, 652.
- [2] D. E. Fenton, J. M. Parker, P. V. Wright, *Polymer* **1973**, *14*, 589.
- [3] J. M. Tarascon, M. Armand, *Nature* **2001**, *414*, 359.
- [4] J. Kim, J. H. Kim, K. Ariga, *Joule* **2017**, *1*, 739.
- [5] W. Xu, J. Wang, F. Ding, X. Chen, E. Nasybulin, Y. Zhang, J. G. Zhang, *Energy Environ. Sci.* **2014**, *7*, 513.
- [6] M. D. Tikekar, S. Choudhury, Z. Tu, L. A. Archer, *Nat. Energy* **2016**, *1*, 16114.
- [7] A. Mauger, M. Armand, C. M. Julien, K. Zaghib, *J. Power Sources* **2017**, *353*, 333.
- [8] J. Mindemark, M. J. Lacey, T. Bowden, D. Brandell, *Prog. Polym. Sci.* **2018**, *81*, 114.
- [9] K. Xu, *Chem. Rev.* **2004**, *104*, 4303.
- [10] J. H. Golden, B. G. M. Chew, D. B. Zax, F. J. DiSalvo, J. M. J. Fréchet, J. M. Tarascon, *Macromolecules* **1995**, *28*, 3468.
- [11] J. Chai, Z. Liu, J. Zhang, J. Sun, Z. Tian, Y. Ji, K. Tang, X. Zhou, G. Cui, *ACS Appl. Mater. Interfaces* **2017**, *9*, 17897.
- [12] S. D. Tillmann, P. Isken, A. Lex-Balducci, *J. Power Sources* **2014**, *271*, 239.
- [13] S. D. Tillmann, P. Isken, A. Lex-Balducci, *J. Phys. Chem. C* **2015**, *119*, 14873.
- [14] J. Zhang, J. Zhao, L. Yue, Q. Wang, J. Chai, Z. Liu, X. Zhou, H. Li, Y. Guo, G. Cui, L. Chen, *Adv. Energy Mater.* **2015**, *5*, 1501082.
- [15] K. Kimura, M. Yajima, Y. Tominaga, *Electrochem. Commun.* **2016**, *66*, 46.
- [16] Y. Tominaga, V. Nanthana, D. Tohyama, *Polym. J.* **2012**, *44*, 1155.
- [17] T. Morioka, K. Nakano, Y. Tominaga, *Macromol. Rapid Commun.* **2017**, *38*, 1.
- [18] L. Meabe, T. V. Huynh, N. Lago, H. Sardon, C. Li, L. A. O'Dell, M. Armand, M. Forsyth, D. Mecerreyes, *Electrochim. Acta* **2018**, *264*, 367.
- [19] H. Xu, H. Zhang, J. Ma, G. Xu, T. Dong, J. Chen, G. Cu, *ACS Energy Lett.* **2019**, *4*, 2871.
- [20] H. Zhang, J. Zhang, J. Ma, G. Xu, T. Dong, G. Cu, *Electrochem. Energy Rev.* **2019**, *2*, 128.
- [21] F. Boujioui, F. Zhuge, H. Damerow, M. Wehbi, B. Améduri, J.-F. Gohy, *J. Mater. Chem. A* **2018**, *6*, 8514.
- [22] M. Yoshikawa, N. Hotta, J. Kyomura, Y. Osagawa, T. Aoki, *Sens. Actuators, B.* **2005**, *104*, 282.
- [23] A. S. Fisher, M. B. Khalid, M. Widstrom, P. Kofinas, *J. Electrochem. Soc.* **2012**, *159*, A592.
- [24] S.-J. Kwon, D.-G. Kim, J. Shim, J. H. Lee, J.-H. Baik, J.-C. Lee, *Polymer* **2014**, *55*, 2799.